Engineering holographic phase diagrams

PHYSICAL REVIEW D **94,** 086004 (2016)

Engineering holographic phase diagrams

Jiunn-Wei Chen,[1,2,*] Shou-Huang Dai,[3,†] Debaprasad Maity,[4,‡] and Yun-Long Zhang[1,§]

[1]*Department of Physics, Center for Theoretical Sciences, and Leung Center for Cosmology and Particle Astrophysics, National Taiwan University, Taipei 10617, Taiwan*

[2]*Center for Theoretical Physics, Massachusetts Institute of Technology, Cambridge, Massachusetts 02139, USA*

[3]*Center for General Education, Southern Taiwan University of Science and Technology, Tainan 71005, Taiwan*

[4]*Department of Physics, Indian Institute of Technology, Guwahati 781039, India*

(Received 8 April 2016; published 10 October 2016)

By introducing interacting scalar fields, we tried to engineer physically motivated holographic phase diagrams which may be interesting in the context of various known condensed matter systems. We introduce an additional scalar field in the bulk which provides a tunable parameter in the boundary theory. By exploiting the way the tuning parameter changes the effective masses of the bulk interacting scalar fields, desired phase diagrams can be engineered for the boundary order parameters dual to those scalar fields. We give a few examples of generating phase diagrams with phase boundaries which are strikingly similar to the known quantum phases at low temperature such as the superconducting phases. However, the important difference is that all the phases we have discussed are characterized by neutral order parameters. At the end, we discuss if there exists any emerging scaling symmetry associated with a quantum critical point hidden under the dome in this phase diagram.

DOI: 10.1103/PhysRevD.94.086004

I. INTRODUCTION

In the modern condensed matter physics, one of the important areas of research is to understand various phases of quantum matter and their transitions. One of the most important examples of such an experimental system with a plethora of phases is the superconducting cuprates. For a conventional (low temperature) superconductor, its many-body ground state and low energy behavior can be described by the Bardeen-cooper-Shrieffer theory [1,2], which is a weakly coupled theory. However, for high temperature superconductors, their superconductivity appears to originate from strongly correlated electrons confined on a two-dimensional plane due to the special molecular structure of the cuprates.

Over the years, many other systems with strong correlation have been discovered, such as the superconducting iron-based compounds known as Pnictides [3]. One of the common features of these systems is the existence of a superconducting dome in the phase diagram. It has become increasingly evident that a significant part of the normal phase right above the dome in these systems, e.g. the strange metal phase, can be described by an emergent conformal field theory (CFT). The CFT is scale free at the quantum critical point where some parameter is tuned to a critical value and the temperature is zero [4,5]. Then, near the critical point, universal, model independent long range physics exists for models within the same universality class which is governed by the deformed CFT with a few symmetry breaking terms. For example, the strange metal behavior exists not only in the high temperature superconductors but also in many-spin systems, e.g. heavy fermion metals [6], near the quantum critical point. The quantum critical point could be hidden or screened by the superconducting dome but revealed by universal low energy behaviors at temperature higher than the dome, such as universal dimensionless transport coefficients which are independent of the microscopic interactions [7].

Since most of these systems are strongly coupled, conventional perturbative QFT is not applicable. Different models are proposed to explain the mechanism; for example, some systems are believed to accommodate competing symmetry-breaking order parameters in a specific range of the physical parameters spanning the phase diagram. Based on this idea of competing orders, many new concepts have been introduced, such as the spin fluctuation superglue [8], the resonating valence bond gauge approach [9,10] and the SO(5) theory [11]. In spite of all these new concepts, and their partial success, full understanding of such systems remains elusive. In view of the nonperturbative nature of the problem, AdS/CFT correspondence [12–14], a tool developed in string theory, provides a new approach to attack the problem.

AdS/CFT correspondence, also called the holographic principle, is a duality between a weakly coupled gravity in anti-di Sitter space (AdS) and a strongly coupled CFT

*jwc@phys.ntu.edu.tw
†shdai.hep@gmail.com
‡debu.imsc@gmail.com
§zhangyunlong@ntu.edu.tw

living on the boundary of the AdS space. This duality spawns a spate of research on a certain class of condensed matterlike systems near the quantum critical point. Over the years, the study in the quantum critical property and the intriguing universal low energy predictions indicates that the universality may have some deep connection with the universal transport properties observed in the normal phase (e.g. the strange metal) of the aforementioned class of real systems [15–17].

AdS/CFT correspondence states that for every particle state in AdS space there exits a dual operator in the corresponding CFT on the boundary. The isometry group of the AdS space is identified with the conformal symmetry of the field theory. This is the symmetry that plays the main role in characterizing various quantum phases and their transitions. One of such phases that has recently been extensively studied at finite charge density is called the "semilocal quantum liquid" [18]. At low energy, this quantum state exhibits different scaling behavior in time and space. Finite temperature phase transition is realized by considering a charged nonextremal black hole in AdS space. In the extremal limit, the zero temperature quantum phase transition of this system is achieved by varying the conformal dimension of the field theory operators. One way to tune the conformal dimension of the strongly coupled operator is by explicitly changing the mass squared of the dual single particle states in a weakly coupled AdS black hole background. However, this way of changing the conformal dimension is not obviously mapped to tuning an experimental parameter from the boundary theory point of view.

Based on the above-mentioned AdS/CFT duality, our main goal in this paper is to construct a minimal bottom-up model that has a similar phase diagram as is observed in high temperature superconductivity. However, let us stress upon the fact that in this paper we are not attempting to construct the actual higher temperature superconducting phase diagram. Our first attempt would be to figure out the most economical way to construct a qualitatively similar phase diagram as the high temperature superconductor. Even though we have successfully constructed such a minimal model, however, we need a certain degrees of fine-tuning to figure out the coupling functions among the scalar fields.

The most basic set for our construction would be to consider a charged black hole which describes a system of finite temperature and chemical potential. Then, we introduce a source J_ϕ for the boundary field theory as a tuning parameter which arises from the near boundary behavior of a dual massive neutral scalar field ϕ in this background. Then, in order to describe the competing phases, we introduce two massive scalar fields $\{\psi_1, \psi_2\}$. For simplicity, both scalars $\{\psi_1, \psi_2\}$ are neutral with no internal quantum number. By choosing the appropriate coupling function between the tuning field ϕ and the order parameter fields $\{\psi_1, \psi_2\}$ in the gravity theory, we can design how the effective masses of $\{\psi_1, \psi_2\}$ depend on J_ϕ at $T = 0$, then engineer various phase diagrams in the $\{J_\phi, T\}$ plane. One can easily generalize this setup to either the $U(1)$ charged field with superconducting condensation or a different kind of antiferromagnetic models, without changing the qualitative behavior of the phase diagram. Study along the similar line has been reported very recently in Ref. [19], where a different system with an extra $U(1)$ gauge field on the gravity background is introduced to represent a chemical potential, as an external tuning parameter for the phase transition in high temperature superconductors. This is an example of modeling the phase transitions in reality due to varying a tunable doping parameter. In the global AdS background, the holographic quantum phase transitions and interacting bulk scalars are also studied in Ref. [20].

This paper is organized as follows. In Sec. II, we introduce the setup and review the holographic properties of the semilocal quantum liquid. In Sec. III, we discuss the engineering of phase diagrams in holography to obtain phase diagrams that are similar to the features of high temperature superconducting cuprates. In Sec. IV, we discuss the scaling symmetries near the quantum region that is not manifest in our models. Our results are summarized and discussed in Sec. V.

II. BACKGROUND GRAVITY

In this section, we review some basic properties of the gravitational background. It has a charged black hole in asymptotic AdS background to describe a system of finite temperature and chemical potential.

Following the work of Refs. [21,22], we introduce the action of the Einstein gravity with Maxwell and other matter fields (which will represent some order parameters in the dual system) in the $3+1$-dimensional bulk,

$$S_{\text{bulk}} = \int \mathrm{d}^4x\sqrt{-g}\left[\frac{1}{2\kappa^2}(R-2\Lambda) - \frac{L^2}{2\kappa^2}\frac{1}{g_F^2}F^2\right] + S_{\text{b.t.}} + \int \mathrm{d}^4x\sqrt{-g}(\mathcal{L}_M) + S_{\text{c.t.}}, \tag{1}$$

where $S_{\text{b.t}}$ and $S_{\text{c.t}}$ denote the boundary terms and the counterterms respectively. The coupling $\kappa^2 = 8\pi G_N/c^4$ is of dimension $[L]^2$, related to the Newton's constant G_N and the speed of light c. The negative cosmological constant is given by $\Lambda = -3/L^2$, where L is the AdS radius. The effective gauge coupling g_F^2 of the Maxwell term is dimensionless.

If we exclude the matter field for now, the Einstein's and Maxwell's equations of motion are

$$R_{\mu\nu} - \frac{1}{2}Rg_{\mu\nu} + \Lambda g_{\mu\nu} = \frac{2L^2}{g_F^2}\left[F_{\mu\lambda}F^{\lambda}{}_{\nu} - \frac{1}{4}F^2 g_{\mu\nu}\right],$$
$$\nabla_\mu F^\mu{}_\nu = 0. \tag{2}$$

The vacuum solution we consider is a charged black brane,

$$ds^2 = \frac{r^2}{L^2}[-f(r)dt^2 + dx^2 + dy^2] + \frac{L^2}{r^2}\frac{dr^2}{f(r)},$$
$$F = g_F\frac{q}{L^2}\frac{r_h^2}{r^2}\mathrm{d}r\wedge\mathrm{d}t, \tag{3}$$

where q is the charge density of the black brane. The factor $f(r)$ and electric potential $A_t(r)$ are

$$f(r) = 1 - (1+q^2)\frac{r_h^3}{r^3} + q^2\frac{r_h^4}{r^4},$$
$$A_t(r) = g_F\frac{qr_h}{L^2}\left(1 - \frac{r_h}{r}\right). \tag{4}$$

We choose the gauge $A_r = 0$, and r_h is the outer horizon of the charged black brane, satisfying $f(r_h) = 0$. According to the standard AdS/CFT dictionary, the temperature and the entropy density of the boundary semilocal quantum liquid are identified as those of the black brane,

$$T = \frac{3}{4\pi}\frac{r_h}{L^2}\left[1 - \frac{q^2}{3}\right], \qquad s = \frac{2\pi}{\kappa^2}\frac{r_h^2}{L^2}. \tag{5}$$

The chemical potential and the charge density are given by [21]

$$\mu_q = g_F q\frac{r_h}{L^2}, \qquad n_q = \frac{2q}{\kappa^2 g_F}\frac{r_h^2}{L^2}. \tag{6}$$

The temperature in (5) can also be expressed in terms of the chemical potential and the position of the outer horizon,

$$T(\mu_q, r_h) = \frac{3}{4\pi}\frac{r_h}{L^2}\left[1 - \frac{1}{3}\frac{L^4}{g_F^2}\frac{\mu_q^2}{r_h^2}\right]. \tag{7}$$

According to the above expression, there are two ways to achieve zero temperature. One is to reduce to pure AdS space, i.e. $r_h = 0$ and $\mu_q = 0$ such that $T(0,0) = 0$, which also implies vanishing charge density. But we are interested in systems with finite density, and therefore we achieve zero temperature by taking the extremal limit of the charged brane $\mu_q^* = \sqrt{3}g_F r_h/L^2$ with nonvanishing r_h, such that $T(\mu_q^*, r_h) = 0$.

The basic guiding principle of AdS/CFT is based on the symmetries on both sides of the correspondence. Scaling symmetry is one of those larger symmetries which plays an important role in understanding the low energy behavior of the system under consideration in terms of relevant operators of the definite scaling dimension. One such interesting system dual to the charged black hole in AdS space is known as the semilocal quantum liquid [18]. Following Ref. [23], we review the scaling symmetries for the semilocal quantum liquids. Our solution is parametrized in terms of two independent parameters q and r_h, while the appropriate physical parameters we consider are temperature T and the chemical potential μ_q. Therefore, in terms of those thermodynamic variables, the equation of state of the dual field theory of the charged black brane turns out to be

$$n_q(\mu_q, T) = \frac{4\pi}{3\kappa^2}\frac{L^2}{g_F^2}\mu_q T\left(1 + \sqrt{1 + \frac{3}{4\pi^2 g_F^2}\frac{\mu_q^2}{T^2}}\right). \tag{8}$$

The equations of motion respect two types of scaling symmetries [24]. The first type is the global scaling

$$L \to aL, \qquad \{r,t,x,y\} \to a\{r,t,x,y\}, \qquad \kappa^2 \to a^2\kappa^2, \tag{9}$$

which rescales the metric $ds^2 \to a^2 ds^2$, and the physical quantities are scaled accordingly,

$$\{T, \mu_q\} \to a^{-1}\{T, \mu_q\}, \qquad \{s, n_q\} \to a^{-2}\{s, n_q\}. \tag{10}$$

One can make use of it to scale away L to unity in the physical quantities, and we will take $L = 1$ in our numerical analysis, meaning every length is measured in units of the AdS radius. The second type is

$$r \to \lambda r, \qquad \{t,x,y\} \to \lambda^{-1}\{t,x,y\}, \tag{11}$$

which leaves ds^2 invariant and the physical quantities

$$\{r_h, T, \mu_q\} \to \lambda\{r_h, T, \mu_q\}, \quad \{s, n_q\} \to \lambda^2\{s, n_q\}. \tag{12}$$

Via this type of scaling, one can initially set horizon size to unit, i.e. $r_h = 1$, for the convenience of computation. In the following numerical analysis, we will set in the beginning $r_h = 1$ for convenience and retain r_h in the equations and diagrams through rescaling it back to the required size afterward. On the other hand, one can redefine the scaling invariant charge density $\tilde{n}_q = (n_q g_F \kappa^2)/(T^2 L^2)$ and chemical potential $\tilde{\mu}_q = \mu_q/(T g_F)$, such that the rescaled equation of state from Eq. (8) is independent of the temperature T,

$$\tilde{n}_q(\tilde{\mu}_q) = \frac{4\pi}{3}\tilde{\mu}_q\left(1 + \sqrt{1 + \frac{3}{4\pi^2}\tilde{\mu}_q^2}\right). \tag{13}$$

A similar scale invariant equation of state in the quantum critical region has been observed in experiments [25,26].

III. PHASE DIAGRAM ENGINEERING

In this section, we would like to construct a minimum holographic model in the bottom-up approach that has a similar phase diagram to a high temperature superconducting cuprate (see, e.g., Fig. 1 of Ref. [27]). As we have already discussed above, at low temperature, distinct phases can be obtained by tuning the doping parameter. In order to understand the basic mechanism of quantum phase transition near zero temperature, we consider interacting order parameter fields.

According to the standard AdS/CFT dictionary, the chemical potential μ_q, conjugate to the charge density n_q, is dual to a bulk gauge field A_μ, such that μ_q and n_q are encoded in the non-normalizable and normalizable modes of the asymptotic behavior of A_μ respectively. Similarly, in our model in this section, the doping parameter should be dual to a bulk scalar field ϕ. In the asymptotic solution of this so-called "tuning field" ϕ, the non-normalizable mode is dual to the source J_ϕ on the boundary, interpreted as the doping parameter since it is an intensive quantity, just like the role of the chemical potential as the non-normalizable mode of the asymptotic A_μ. The normalizable mode of ϕ, on the other hand, is dual to the expectation value of the conjugate variable to the doping parameter, which we do not specify.

We consider two order parameter fields to be neutral scalar fields ψ_1, ψ_2 in the AdS bulk. We also conjecture that the controlling parameter of our system is dual to another neutral field ϕ which is coupled to ψ_1, ψ_2 with a certain degree of fine-tuning, such that we can reproduce the experimental phase diagram.

Our goal is to understand the phase diagram and the scaling behavior near the quantum critical point in such a system. In order for the two order parameters to be controlled by tuning the external parameter, it requires ψ_1, ψ_2 to interact with the tuning field ϕ in some nonlinear way. Therefore, we introduce the following minimal Lagrangian density,

$$\mathcal{L}_M = \sum_{i=1,2} \mathcal{L}_{\psi_i} + \mathcal{L}_\phi + \mathcal{L}_{\rm int}, \tag{14}$$

where

$$\begin{aligned} g_M^2 \mathcal{L}_{\psi_i} &= -\frac{1}{2}(\partial\psi_i)^2 - V(\psi_i), \\ V(\psi_i) &= \frac{1}{2} m_i^2 \psi_i^2 + \frac{1}{4}\lambda_i \psi_i^4, \end{aligned} \tag{15}$$

$$\begin{aligned} g_M^2 \mathcal{L}_\phi &= -\frac{1}{2}(\partial\phi)^2 - V(\phi), \\ V(\phi) &= \frac{1}{2} m_\phi^2 \phi^2 + \frac{1}{4}\lambda_\phi \phi^4, \end{aligned} \tag{16}$$

with g_M^2 indicate the coupling constant, m_i^2, $m_\phi^2 < 0$ and λ_i, $\lambda_\phi > 0$. The interaction terms between ψ_1, ψ_2 and ϕ are given by

$$g_M^2 \mathcal{L}_{\rm int} = -\frac{1}{2}\sum_{i=1,2} F_i(\phi)\psi_i^2, \tag{17}$$

where the detailed form of the coupling function $F_i(\phi)$ will be given later. Different $F_i(\phi)$ implies different ways in which the condensation of ψ_1 and ψ_2 are controlled by ϕ via shifting their effective masses. Consequently, different phase structures arise. We will work in the probe limit of the scalar fields, namely $2\kappa^2/g_M^2 \to 0$.

The equations of motion for the scalar fields turn out to be

$$0 = r^{-2}\partial_r[r^4 f(r)\partial_r\psi_i] - [m_i^2 + F_i(\phi)]\psi_i - \lambda_i\psi_i^3, \tag{18}$$

$$0 = r^{-2}\partial_r[r^4 f(r)\partial_r\phi] - m_\phi^2\phi - \frac{1}{2}\sum_{i=1,2} F_i'(\phi)\psi_i^2 - \lambda_\phi\phi^3. \tag{19}$$

It is clear from these equations that the tuning field ϕ shifts the effective mass of ψ_i from m_i^2 to

$$\tilde{m}_i^2(r) = m_i^2 + F_i(\phi(r)). \tag{20}$$

According to the argument in Ref. [18], when the mass square near the horizon is below the Breitenlohner-Freedman (BF) bound of AdS_2 that $\lim_{r\to r_h}\tilde{m}_i^2(r) < -3/2$, there will be a phase transition near zero temperature. In order to keep the stability near the AdS_4 boundary, one also needs to keep the mass square near the boundary above the BF bound of AdS_4 that $\lim_{r\to\infty}\tilde{m}_i^2(r) > -9/4$. In the phase diagram, we also need to map the horizon value $\phi(r_h)$ into the quantity J_ϕ of the dual field.

At finite temperature, the near horizon expansions of the scalar fields are

$$\psi_i(r) = \psi_i(r_h) + \psi_i'(r_h)(r - r_h) + \cdots, \tag{21}$$

$$\phi(r) = \phi(r_h) + \phi'(r_h)(r - r_h) + \cdots, \tag{22}$$

and solving the equation of motion leads to

$$\psi_i'(r_h) = [m_i^2\psi_i(r_h) + \lambda_i\psi_i(r_h)^3]/(4\pi T), \tag{23}$$

$$\phi'(r_h) = \left[m_i^2\phi(r_h) + \lambda_i\phi(r_h)^3 + \frac{1}{2}\sum_i F_i'(\phi)\psi_i^2\right]/(4\pi T). \tag{24}$$

These formulas are used to evaluate the scalar field in the numerical analysis once the boundary values on the horizon

are specified. On the other hand, the asymptotic forms are given by

$$\psi_i(r) \to \frac{J_i}{r^{\Delta_i^-}} + \frac{O_i}{r^{\Delta_i^+}}, \qquad \Delta_i^{\pm} = \frac{3}{2} \pm \sqrt{\frac{9}{4} + m_i^2}, \tag{25}$$

$$\phi(r) \to \frac{J_\phi}{r^{\Delta_\phi^-}} + \frac{O_\phi}{r^{\Delta_\phi^+}}, \qquad \Delta_\phi^{\pm} = \frac{3}{2} \pm \sqrt{\frac{9}{4} + m_\phi^2}. \tag{26}$$

From the above Eqs. (25) and (26) of the asymptotic behavior of the bulk fields, one can obtain the scaling dimension of the dual boundary operators, $(O_i,\ O_\phi)$ and their conjugates, $(J_i,\ J_\phi)$ as

$$\{J_i, J_\phi\} \to \{\lambda^{\Delta_i^-} J_i, \lambda^{\Delta_\phi^-} J_\phi\},$$
$$\{O_i, O_\phi\} \to \{\lambda^{\Delta_i^+} O_i, \lambda^{\Delta_\phi^+} O_\phi\}. \tag{27}$$

In our analysis, we choose the standard quantization on the boundary for the asymptotic ψ_i, that set the boundary source $J_i = 0$. Therefore, we do not need to consider the correction term in asymptotic ψ_i due to ψ_i^4 self-interaction in (A11). The cross-interaction $F_i(\phi)\psi_i^2$ will not incur corrections to either asymptotic ψ_i or ϕ due to the same reason. The ϕ^4 interaction induces correction to the asymptotic ϕ solution, but we will constrain the mass of ϕ to $m_\phi^2 < -27/16$ in our analysis, so that the correction contributes at the subleading order in the normalizable mode and can be neglected at asymptotic infinity.

In the following, we present two different models, with different sets of $\{m_i^2, m_\phi^2, \lambda_i, \lambda_\phi\}$ parameters and the coupling functions $F_i(\phi)$. As expected, tuning the source parameter J_ϕ (which is the non-normalizable mode of ϕ) leads to a different phase diagram. Such phenomena have been observed in the phase diagrams of high temperature superconductors.

To check the thermodynamic stability of any particular phase, we need to examine the free energy of the condensed state and normal state in the ordered phase (see more details in Appendix A). The free energy densities with and without ψ_i in these states are given by

$$\frac{\Delta\Omega}{V_{(2)}} = \frac{\Delta\Omega_\phi}{V_2} - \frac{1}{4g_M^2}\int_{r_h}^{\infty} \mathrm{d}r \frac{r^2}{L^2}\sum_i [\lambda_i \psi_i^4 + \phi F_i'(\phi)\psi_i^2], \tag{28}$$

$$\frac{\Delta\Omega_\phi}{V_2} = -\frac{\lambda_\phi}{4g_M^2}\int_{r_h}^{\infty} \mathrm{d}r \frac{r^2}{L^2}(\phi^4), \tag{29}$$

where the free energy coming from the pure black brane background has been subtracted. In the subsequent subsections, we will study two possible phase diagrams by tuning the temperature and the source parameter J_ϕ and checking the free energies to shed light on the possible ground states for a given value of $\{J_\phi, T\}$.

A. Model I with positive doping parameter

In this model, we engineer a phase diagram with two condensed phases mimicking the antiferromagnetic phase and the pseudogap phase. In the Lagrangian density (14), we choose the following coupling functions $F_1(\phi)$ and $F_2(\phi)$,

$$-F_2(\phi) = \phi^2 - \frac{5}{24}\phi^4 \cong F_1(\phi). \tag{30}$$

To avoid the instability of the scalar fields due to the unboundedness from below in the potential in (17) and (30), we can add a small ϕ^6 term to $F_1(\phi)$, e.g. $F_1(\phi) = \phi^2 - 5\phi^4/24 + \phi^6/100$. This will only change the full phase diagram slightly. Our choice is tuned to that particular form, so that we can construct a phase diagram which mimics the phase boundary of high temperature superconductors. Moreover, this choice also reduces the complication in numerical analysis. We also choose the following set of parameters:

$$m_1^2 = -2.1, \qquad \lambda_1 = 2,$$
$$m_2^2 = -1.0, \qquad \lambda_2 = 2,$$
$$m_\phi^2 = -1.8, \qquad \lambda_\phi = 1/3. \tag{31}$$

Together with the boundary condition for ψ_i at asymptotic infinity such that $J_i = 0$, the correction terms due to the self- and cross-interaction terms drop out, as explained below Eq. (27).

The asymptotically AdS boundary keeps $\lim_{r\to\infty}\phi(r) = 0$, and with the coupling functions in (30), we have $\lim_{r\to\infty} F_i(\phi(r)) = 0$. According to the effective masses in Eq. (20), our parameters in (31) always meet with the stable condition near the boundary of AdS_4 at which $\lim_{r\to\infty}\tilde{m}_i^2(r) > -9/4$. On the other hand, the effective masses of the scalar fields near the horizon are

$$\tilde{m}_1^2(r_h) = -2.1 + \left[\phi(r_h)^2 - \frac{5}{24}\phi(r_h)^4\right], \tag{32}$$

$$\tilde{m}_2^2(r_h) = -1.0 - \left[\phi(r_h)^2 - \frac{5}{24}\phi(r_h)^4\right]. \tag{33}$$

Therefore, if we tune the value of $\phi(r_h)$ at zero temperature, there will be a phase transition when the effective mass square near the horizon crossing the BF bound of AdS_2 that $\tilde{m}_i^2(r_h) = -3/2$. Additionally, the parameters of scalar field ϕ are chosen to keep a monotonous relation between $\phi(r_h)$ and J_ϕ, which maps the phase transition parameter $\phi(r_h)$ into the quantity J_ϕ of the dual field.

In Fig. 1, we first plot the expectation value of the dual operator O_ϕ with the color gradient on the rescaled $\{J_\phi, T\}$ plane. We only consider the J_ϕ parameter over a small positive range in this diagram. The location of

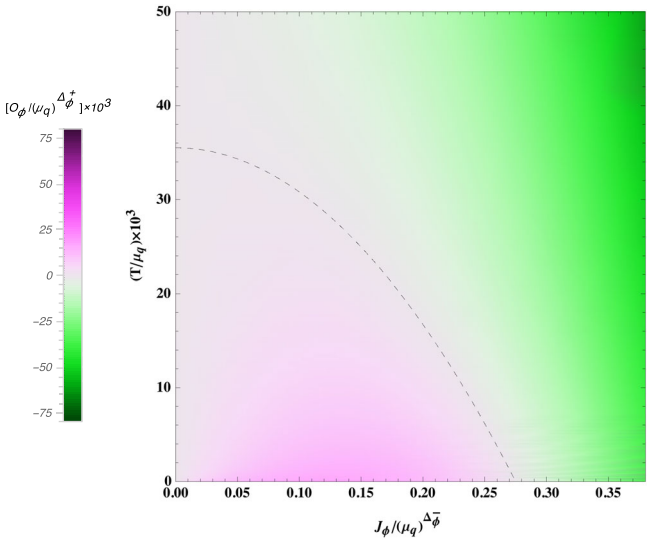

FIG. 1. The density plot for the expectation value of O_ϕ vs the rescaled temperature T/μ_q and the rescaled doping parameter (the source) $J_\phi/(\mu_q)^{\Delta_\phi^-}$, both by appropriate power in the chemical potential μ_q. The dotted line is where O_ϕ vanishes. Note that O_ϕ is nonvanishing in general. And the relation between O_ϕ and J_ϕ is similar to the "equation of state" of the doping matter dual to scalar field ϕ.

vanishing O_ϕ varies with J_ϕ, indicated by the dashed line in the figure. In terms of the order parameter O_ϕ, there is no phase transition across the dashed line. It would be very interesting if there were a phase transition in O_ϕ as it would provide a way to describe the pseudogap as we will discuss in Sec. IV.

Now, we turn on the fields ψ_1 and ψ_2; the phase diagram of this system is presented in Fig. 2. It contains two distinct ordered phases, characterized by nontrivial values of O_1 and O_2 respectively, besides the normal one. This diagram

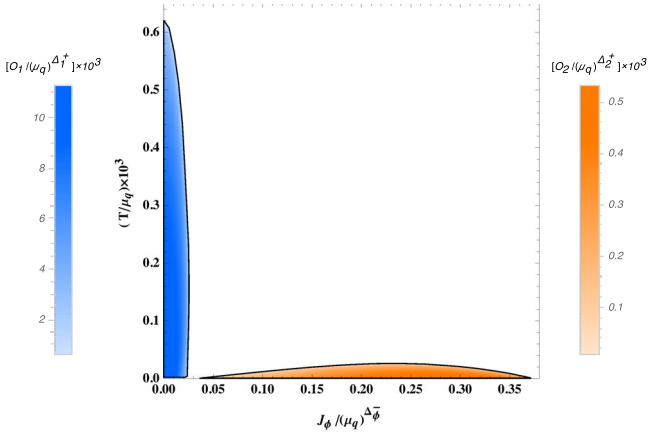

FIG. 2. The phase diagram of model I with positive doping parameter. It is the density plot for phase 1(blue) and phase 2 (orange) with coupling functions $-F_2(\phi)=\phi^2-5\phi^4/24\cong F_1(\phi)$.

is obtained by setting the sources of ψ_1 and ψ_2 on the boundary to zero but turning on the boundary source J_ϕ of scalar field ϕ and the background temperature.

In this phase diagram, we only consider a small range of positive rescaled J_ϕ. The ordered phase 1 (in blue color) occurs at low J_ϕ and extends up to higher temperature, while the dome-shape ordered phase 2 (in orange color) covers the low temperature region down to $T=0$, over a finite range of positive J_ϕ. This feature is qualitatively similar to the phase boundary in the phase diagram of the cuperate superconductors. If one wishes to create a more realistic model and identify the ordered phase 1 (characterized by nontrivial O_1) near $J_\phi=0$ to the antiferromagnetic phase of the cuperates, one needs to generalize ψ_1 to be one component of the $SU(2)$ multiplet [18]. This in principle requires including other components of $SU(2)$ in the Lagrangian but only allows ψ_1 to condense. Further, in order to have more realistic phase diagram, the order parameters can also be coupled with extra $U(1)$ gauge field. Since the goal of this paper is to explore the possibility of forming different phases via the tuning field ϕ and the coupling function $F_i(\phi)$, the study of the more realistic model can be left for future work.

Figure 3 shows that the ordered phase 1 and phase 2 are indeed thermodynamically preferred, by comparing the free energy density of the solutions with and without the condensate in the range of J_ϕ in those phases at a fixed temperature. The difference of free energy density is based

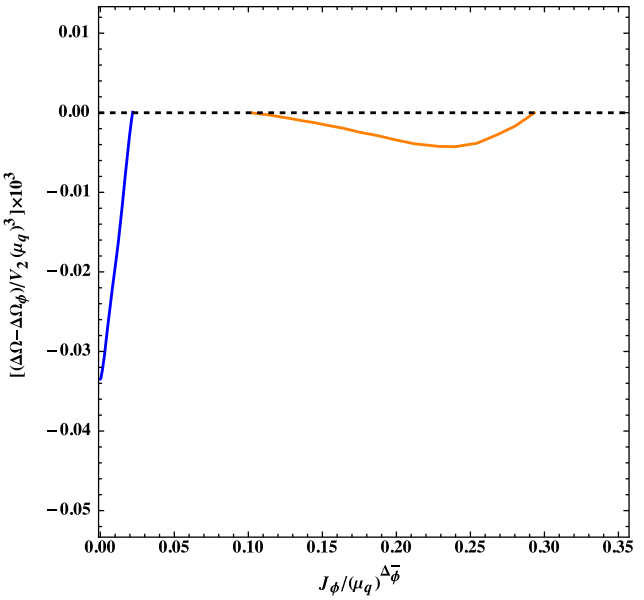

FIG. 3. The free energy density difference between the ordered and normal phases. The rescaled temperature is chosen as $(T/\mu_q)\simeq 0.014\times 10^{-3}$. The dashed black line stands for the baseline of the free energy of the normal phase with only the ϕ condensate. The blue and orange lines correspond to the free energy difference of phase 1 and phase 2, respectively.

on formulas (28) and (29), and here we only show the free energy density difference $\Delta\Omega - \Delta\Omega_\phi$ at a particular value $(T/\mu_q) \simeq 0.014 \times 10^{-3}$. The blue and orange lines correspond to the free energy difference of phase 1 and phase 2, respectively. And the dashed black line stands for the baseline of the free energy of the normal phase with only the ϕ condensate.

B. Model II with competing orders

In this model, we have a region with two condensates coexisting which provides a model to study the physics of competing orders. The phase diagram is also similar to the region with a dome and a pseudogap phase. We start with the following simple choices of parameters in the Lagrangian density (14),

$$\begin{aligned} m_1^2 &= -1.5, \qquad \lambda_1 = 2, \qquad F_1(\phi) = \phi(\phi+2) \\ m_2^2 &= -1.9, \qquad \lambda_2 = 2, \qquad F_2(\phi) = \phi^2/2 \\ m_\phi^2 &= -1.5, \qquad \lambda_\phi = 0. \end{aligned} \tag{34}$$

Similar to the arguments around Eq. (32), our parameters in Eq. (34) always meet with the stable condition near the boundary of AdS_4 at which $\lim_{r\to\infty}\tilde{m}_i^2(r) > -9/4$. On the other hand, the effective masses of the scalar fields near the horizon are

$$\tilde{m}_1^2(r_h) = -1.5 + \phi(r_h)(\phi(r_h)+2), \tag{35}$$

$$\tilde{m}_2^2(r_h) = -1.9 + \phi(r_h)^2/2. \tag{36}$$

When above effective masses cross the BF bound of the AdS_2, we will have phase transition at zero temperature, provided one maintains a monotonic relation between $\phi(r_h)$ and J_ϕ.

We define the normal phase of our system with all the order parameter fields $\psi_i = 0$, which is to say that there is no condensation of the corresponding dual field theory operator. Therefore, the system is in the completely symmetric phase. We numerically study how different possible phases and their transitions are occurring as we go toward the zero temperature limit for different values of the source parameter J_ϕ at the boundary field theory. In this case, we assume the tuning parameter taking both negative and positive values, which mimics the electron and hole doping into the system for the high temperature superconductor. Therefore, the $J_\phi = 0$ can be identified as the quantum critical point where the transition temperature is zero. The other motivation of the choices of parameters in this model refers to the phase diagrams in Ref. [28], which is related with at zero source J point through scaling symmetries. But for our specific choices of parameters, we see from phase diagram 4 that the quantum critical point is covered by a dome with nonzero condensation of $O_2 \neq 0$,

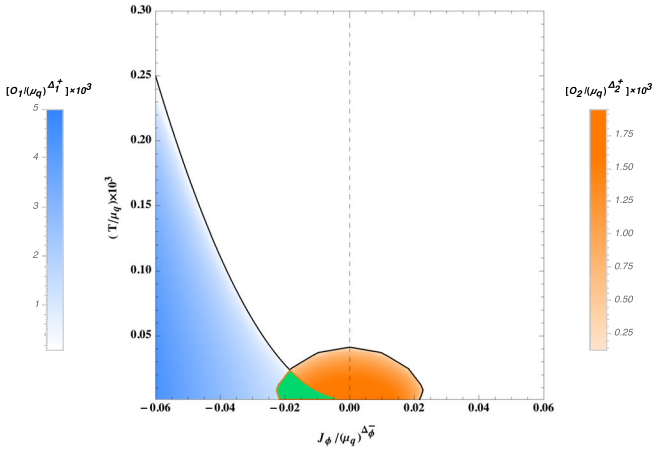

FIG. 4. The phase diagram of model II around a natural quantum critical point. It is the density plot phase 1 (blue) and phase 2 (orange) with coupling functions $F_1(\phi) = \phi(\phi+2)$, $F_2(\phi) = \phi^2/2$. The green parts are the overlap region.

which normally happens in real physical systems. One also notices that there exists an overlapping phase which we left for future studies.

Once we numerically compute various condensations for the different phases, one needs to compare the free energy among various phases in Fig. 4. As we have calculated the free energy for various phases, in Fig. 5, we have plotted them using the expressions (28) and (29). We show the free energy density difference $\Delta\Omega - \Delta\Omega_\phi$ at a particular value $(T/\mu_q) \simeq 0.028 \times 10^{-3}$. The blue and orange lines

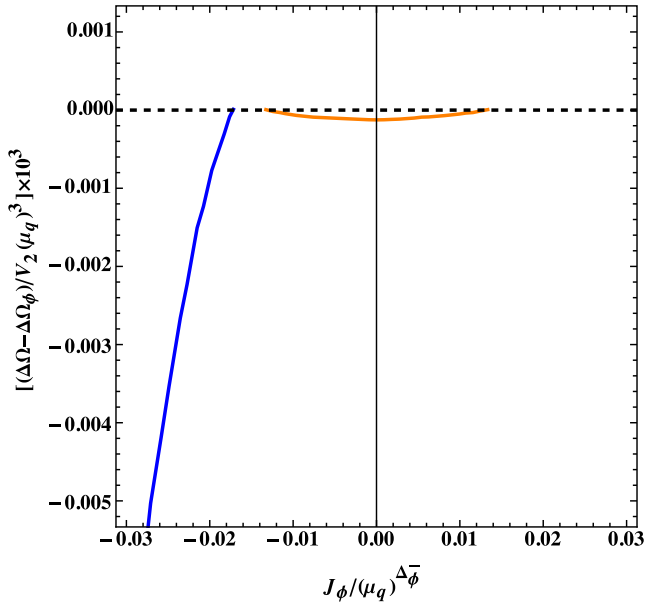

FIG. 5. The energy difference between the ordered and normal phases in Fig. 4 at $(T/\mu_q)\times10^3 \simeq 0.028$. The dashed black line stands for the baseline of the free energy of the normal phase with only the ϕ condensate. The blue and orange lines correspond to the free energy difference of phase 1 and phase 2, respectively.

correspond to the free energy difference of phase 1 and phase 2, respectively. And the dashed black line stands for the baseline of the free energy of the normal phase with only the ϕ condensate.

One notices that in the region $J_\phi < 0$, $\Delta\Omega - \Delta\Omega_\phi < 0$. Therefore, the ground state of the system will be in the phase with $O_1 \neq 0$. On the other hand, near the $J_\phi = 0$ region, we found that the free energy $\Delta\Omega$ becomes almost comparable to $\Delta\Omega_\phi$, as one sees from Fig. 5. But still $O_2 \neq 0$ is preferable near the $J_\phi = 0$, $T = 0$. The green region is the overlap region, and usually there exist some competing and coexistence orders; see, e.g., Refs. [29–35]. This region is not the main purpose of our model, and it would be interesting to explore more on this issue in future work.

IV. TOWARD A MORE REALISTIC PHASE DIAGRAM

From our toy model to a more realistic holographic model of a high temperature superconductor, we need at least the following improvements: (a) realistic condensates for the antiferromagnetic and superconducting phases, (b) a pseudogap phase, and (c) scaling symmetry associated with the screened quantum critical point below the superconducting dome.

For (a), it is not difficult to replace ψ_1 of model I by a condensate that has $SU(2)$ components to make it a realistic antiferromagnetic phase [18,36]. It is also not difficult to replace ψ_2 of the same model by a complex scalar field coupled to the bulk $U(1)$ gauge field in Eq. (1) to have a S-wave superconductor, or different kinds of holographic P-wave superconductors [37–41]. However, experimentally, the condensate for the superconductor is of the D-wave. Naively, one might expect that this can be achieved by just employing a symmetric traceless second rank tensor as the order parameter field in the bulk. However, this naive construction has more components than needed which need to be removed in a general covariant way. The fact that this field is charged and massive in the AdS background makes things even more complicated [42]. This is the difficulty of constructing high spin field theory. It is a long-standing problem and is not yet resolved despite lots of efforts [43–45]. Additionally, it is also an ingredient to introduce the momentum dissipation under the dome shaped region [46,47].

In the following subsections, we discuss the missing pseudogap phase and scaling symmetry in our phase diagram Fig. 2 or Fig. 4, which is based on the models presented in Sec. III.

A. Pseudogap phase

The definition of a pseudogap phase is where the fermion spectral function has a gap but the order parameter is zero. For cuprate superconductors, the pseudogap phase occurs at the temperature T_* above the superconductor phase transition T_c ($T_* > T_c$), where the superconducting order parameter vanishes, but the gap in the fermionic spectral function remains finite.

A holographic pseudogap model has been realized in Refs. [48,49]. However, the order parameter field that couples to fermions to generate the gap in the fermionic spectral function is also the one characterizing the superconductor phase. As a result, when the order parameter vanishes, the gap disappears. Therefore, the pseudogap phase appears at the temperature below the superconductor transition ($T_* < T_c$). This problem can be solved in the expanse of introducing another field to generate a condensate that gives a gap to the fermion spectral function (analogous to Ref. [19]), while the condensate of another field is responsible for generating superconductivity. The explicit model was constructed as our model II. However, it would be more economical if we could use the field ϕ to do this job of generating a gap in the fermionic spectral function. Unfortunately, we have not succeeded in engineering a generic phase transition for ϕ; otherwise, using fields ϕ, ψ_1, and ψ_2, we would be able to generate the antiferromagnetic, superconducting, and pseudogap phases using the setup of model I.

B. Scaling symmetry in (μ_q, T) space with $J_\phi = 0$

Scaling symmetry is an important feature of the phase diagram of a high temperature superconductor which suggests there is a quantum critical point hidden under the superconducting dome. The physics of the scaling symmetry can be understood from effective field theory. At the critical point, the theory is scale invariant such that the theory has no scale in the problem. Away from the critical point, the theory does not have exact scaling symmetry, but it is broken softly, and the breaking can be computed in terms of the soft symmetry breaking parameter(s). Therefore, near the quantum critical point, the symmetry breaking at different points of phase space can be related by scaling. This is the scaling symmetry governed by the existence of the quantum critical point. A prime example of this type of scaling is the strange metal phase.

In the context of AdS/CFT, a similar scaling symmetry has been discussed in holographic superconductor model [37]. As reviewed in Appendix B, the order parameter vs temperature relation can be plotted in scaling invariant parameters as in Fig. 9. This plot is redrawn in Fig. 6 to demonstrate the scaling symmetry; once the physics on a constant T slice is known, then the physics at all T is known. The dashed lines on this plot show physics on this line can be obtained by scaling. This is a nice demonstration that physics away from the quantum critical point at the origin is related to physics near the quantum critical point. It is also interesting to consider the condensed phase in dilaton gravity where the scale invariance is broken [50,51].

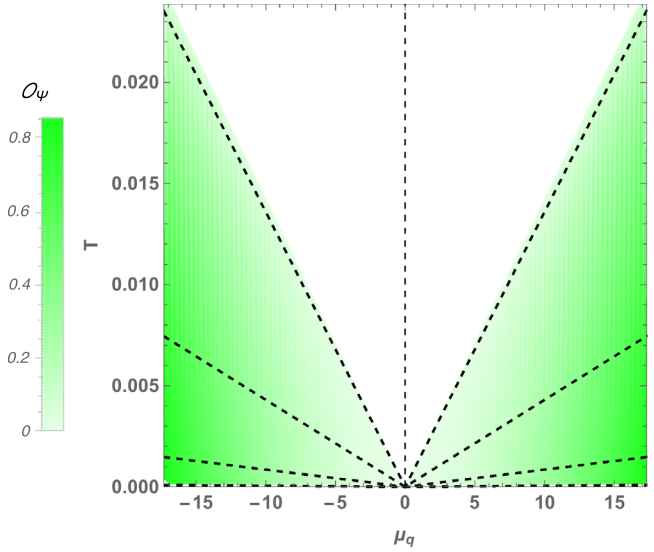

FIG. 6. The density plot of the order parameter O_Ψ on the $\{\mu_q, T\}$ plane, which is equivalent to Fig. 9 of a single charged scalar field model in Appendix B. The transparent middle region has vanishing order parameter and is the normal phase, where the equation of state $\tilde{n}_q(\tilde{\mu}_q)$ in Eq. (13) is independent of the temperature. There are two condensed phases: the right-hand side one has a positive charge density n_q, while the left-hand side one has a negative n_q. The dashed lines indicate the scaling trajectories. Note that this toy model has scaling symmetry even in the condensed phases. In this figure, we have set $g_F = 1$, $L = 1$ for convenience.

The scaling symmetry in Fig. 6 seems to capture the essence of scaling symmetry in superconductors although it is known that the probe limit fails near zero temperature [52,53]. On the other hand, some new ground state, such as the AdS soliton background [54,55], which is dual to an insulating phase, may appear and hence break the scaling symmetry [18,56].

In our phase diagrams shown in Figs. 2 and 4, there is also scaling with respect to physics of different μ_q which has the same origin with the HHH model mentioned above which also has a powerful scaling symmetry for the condensates. However, the scaling symmetry in the T–J_ϕ plan is not manifest, as μ_q is assumed constant on the phase diagram. It is possible that by shrinking the dome phase to a point certain scaling symmetry on the T–J_ϕ can emerge from the effective field theory argument. But apparently this cannot be seen easily through the bulk asymptotic equation of motion near the boundary.

C. Aspect of scaling symmetry in (J_ϕ, T) space

In Sec. III, all the figures are plotted in terms of scale invariant quantities, as the usual strategy of presenting figures in holographic superconductors [23,39]. However, in the figures of the condensed matter experiment [25,26], the obvious scaling symmetry only exists in the V-shape quantum critical region. In this section, we use the schematic diagram to show the scaling symmetries in our models.

After adding the doping field ϕ, we have three independent parameters $\{\mu_q, J_\phi, T\}$ in the dual boundary system. In order to see the obvious scaling symmetry similar to that in Fig. 6, we need to transform our Figs. 2 and 4 into three-dimensional figures in terms of $\{\mu_q, J_\phi, T\}$. In the following, we only plot the schematic diagrams, and we introduce the notation $\tilde{J}_\phi \equiv (\mathrm{Sign}[J_\phi])|J_\phi|^{1/\Delta_\phi^-}$ instead of J_ϕ.

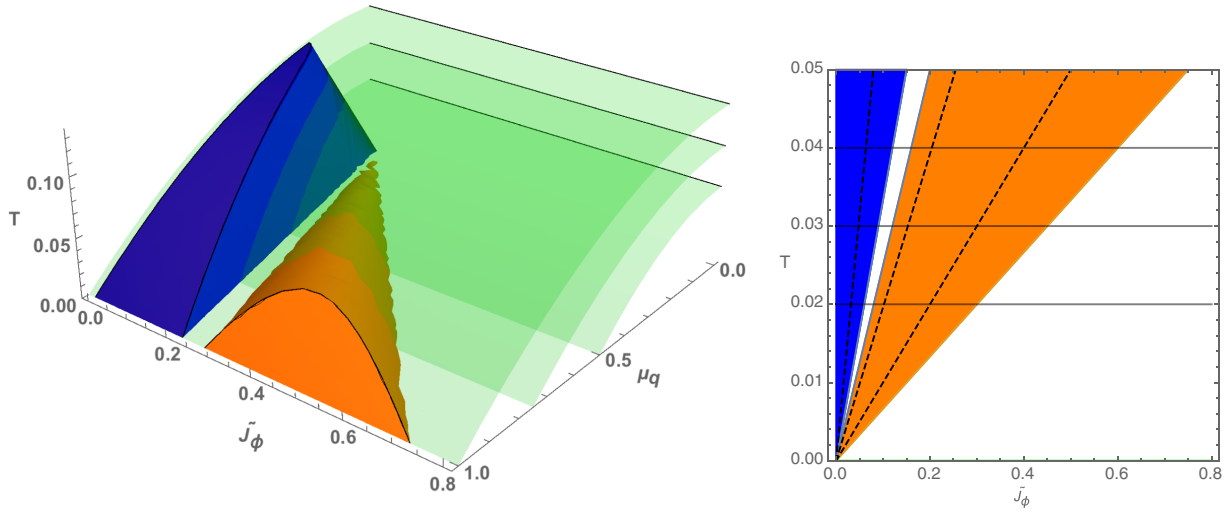

FIG. 7. Left: the 3D schematic diagram of Fig. 2 in terms of $\{\mu_q, \tilde{J}_\phi, T\}$, where the blue and orange regions correspond to ordered phase 1 and phase 2. Three light green surfaces indicate parameter constraints of constant r_h. Right: Phase diagram in terms of $\{T, \tilde{J}_\phi\}$ at a fixed μ_q/T cross-profile, which corresponds to fixing the parameter q in (5). The dashed line indicates the scalings, and the solid gray line indicates the parameter constraint of constant r_h.

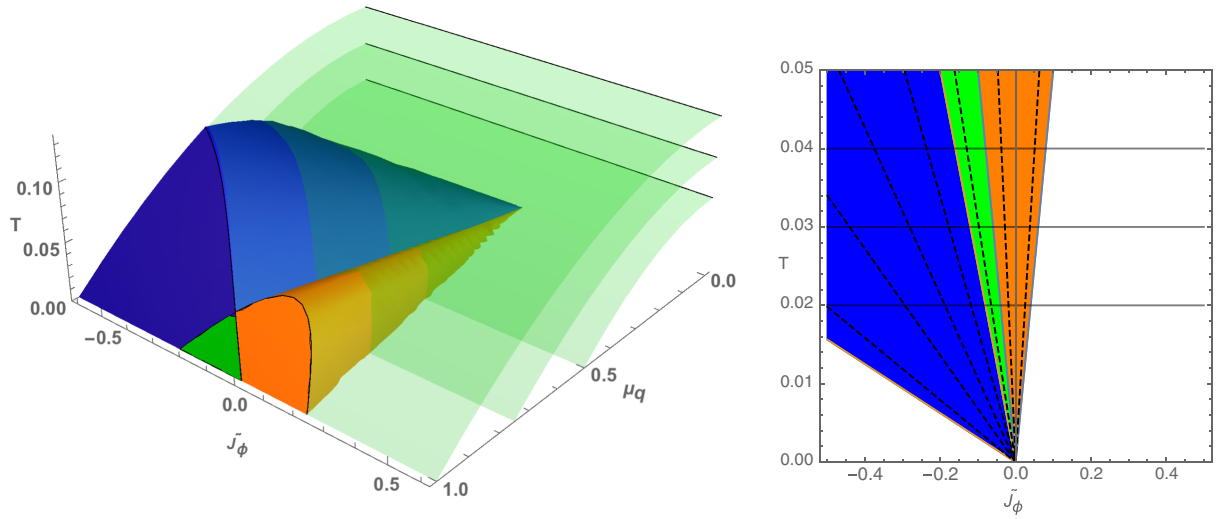

FIG. 8. Left: the 3D schematic diagram of Fig. 4 in terms of $\{\mu_q, \tilde{J}_\phi, T\}$, where the blue, orange and green regions correspond to ordered phase 1, phase 2 and the overlap phase. Three light green surfaces indicate the parameter constraint of constant r_h. Right: Phase diagram in terms of $\{T, \tilde{J}_\phi\}$ at a fixed μ_q/T cross profile, which corresponds to fixing the parameter q in (5). The dashed line indicates the scalings, and the solid gray line indicates the parameter constraint of constant r_h.

As indicated in Figs. 7 and 8, the different color shapes correspond to different ordered phases. The blue region is phase 1, and the orange region is phase 2. And the three light green surfaces indicate the parameter constraint of constant r_h. In more detail, if we assume $\tilde{T} = T/r_h$, $\tilde{\mu}_q = \mu_q/r_h$, then from relation (7) we obtain $\tilde{T} = \frac{3\pi}{4}(1 - \tilde{\mu}_q^2/3)$. This indicates that $\tilde{T}$ and $\tilde{\mu}_q$ are not independent anymore. The light green surfaces indicate the constraint relation between $T = \tilde{T} r_h$ and $\mu_q = \tilde{\mu}_q r_h$, with three different constants r_h. The two-dimensional phase diagram crossed by different light green surfaces can be related through scaling along with r_h.

Our 3D diagrams in this section are similar to Fig. 14 in Ref. [28]. Although we introduce the external scaler fields in probe limit, our whole system still has the scaling symmetries the near $J_\phi = 0$. However, in the real condensed matters systems, the scaling symmetry only exists in the V-shape quantum critical region, which is generally at nonzero critical doping parameter. It is destroyed at very large J and large T. Therefore, it would be interesting find out some mechanism which will provide such scaling for nonzero doping in the holographic context.

V. CONCLUSION AND DISCUSSION

We have studied how to engineer holographic models with features similar to a high temperature superconductor phase diagram. We introduce a field ϕ in the bulk which provides a tunable "doping" parameter J_ϕ in the boundary theory. By designing how this field changes the effective masses of other order parameter fields, desired phase diagrams can be engineered. We have given examples of generating phase diagrams with phase boundaries similar to a superconducting dome and an antiferromagnetic phase by including two order parameter fields ψ_1 and ψ_2.

It's straightforward to change our scalar fields ψ_1 and ψ_2 into well-studied models of holographic antiferromagnetic and superconductors. However, the shape of our phase diagram will not change, as the basic underlying mechanism of phase transition is the same in the holographic models. As we have also mentioned before, the perturbation of the scalar field near the horizon region becomes unstable, and a hairy solution with scalar field is perfected due to lower free energy. More detailed evidence can be found in Ref. [18].

It is well known that the holographic phase transition is based on the violation of the BF bound in the near horizon AdS_2 region as explained in Ref. [18]. It is strikingly similar to the phase transition phenomena in Ginzburg-Landau theory. Usually in the holographic context, changing the temperature of a black hole effectively changes the effective mass of an order parameter field under consideration, and this leads to a spontaneous symmetry breaking and consequently the phase transition. However, in our present case, we have an additional tuning parameter which is the source term of a scalar field in the bulk. Therefore, even with fixed temperature, we can control the effective mass of the order parameter field coupled with the tuning parameter J_ϕ field and hence violate the BF bound. Therefore, we can have the interesting phase diagram in (T, J_ϕ) space as shown in Figs. 2 and 4. As we have extensively discussed, choosing different coupling functions for the tuning field with the order parameter fields can provide us different phase diagrams depending upon the requirement of a real system.

Finally, we would like to emphasize the difference between our minimal model and the model in Ref. [19]. Instead of using the specific holographic models of superconductor and anti ferro-magnetism as in Ref. [19], our model provides a simpler picture to engineer the holographic phase diagrams based on the setup in Ref. [18]. In our model I, the coupling functions $F_1(\phi) = -F_2(\phi)$ are enough to change the effective mass of scalar fields ψ_1 and ψ_2, with less parameter choice to obtain the desired shapes. In principle, we can also add and engineer other phases with different shapes in the phase diagrams. Moreover, instead of considering additional U(1) gauge field as the doping parameter, we simply choose a scalar field ϕ, with a free parameter m_ϕ to change the scaling dimensions of the tuning source J_ϕ and conjugate physical momenta O_ϕ. Thus, our source field has more freedom to be connected with other tuning fields in the phase diagrams, such as the massive field, external magnetic field and pressure induced space changing in the experiment. Additionally, for our model II, we have the freedom to realize different phase diagrams in the positive and negative tuning parameter regions, through changing the coupling function $F_i(\phi)$.

ACKNOWLEDGMENTS

This work is supported by the MOST, NTU-CTS and the NTU-CASTS of Taiwan.

APPENDIX A: FREE ENERGY DENSITY

In this section, we calculate the contribution to the free energy from the background gravity, the Maxwell field and the probe scalar fields. We will also follow this approach in Sec. III for our model to understand the stability of all possible phases against each other.

In a grand canonical ensemble, the Gibbs free energy Ω is obtained from the partition function. In the AdS/CFT correspondence and the semiclassical limit, the partition function of the bulk theory is the path integral over the Euclidean metrics

$$\Omega = T \log Z, \qquad Z = -\exp\left(-S^{(E)}_{\text{total}}\right), \tag{A1}$$

where the Euclidean action is obtained via the Wick rotation

$$\tau = it, \qquad \tau \sim \tau + T^{-1}. \tag{A2}$$

To fulfill our purpose, we mainly follow Ref. [23]. With a Dirichlet-like conformally flat boundary at infinity, the Euclidean action of the bulk Einstein-Maxwell theory is [57–59]

$$S^{(E)}_R = -\int \mathrm{d}r \int \mathrm{d}\tau \mathrm{d}^2x \sqrt{g}\left[\frac{1}{2\kappa^2}\left(R + \frac{6}{L^2}\right) - \frac{L^2}{2\kappa^2}\frac{1}{g_F^2}F^2\right] + S_{\partial\mathcal{M}}, \tag{A3}$$

where $S_{\partial\mathcal{M}}$ contains the well-known Gibbons-Hawking term for the well-defined variational problem and a constant boundary counterterm to cancel the divergence of the bulk action,

$$S_{\partial\mathcal{M}} = \int_{r\to\infty} \mathrm{d}\tau \mathrm{d}^2x \sqrt{h} \times \left[\frac{1}{2\kappa^2}\left(-2K + \frac{4}{L}\right) + \frac{2L^2}{\kappa^2}\frac{\varepsilon}{g_F^2} n^a F_{ab} A^b\right]. \tag{A4}$$

Here, h is the induced metric on boundary at $r \to \infty$, and $K = h_{\mu\nu}\nabla^\mu n^\nu$ is the trace of the extrinsic curvature of the boundary hypersurface, with n^μ an outward pointing unit normal vector. $\varepsilon = 0$ corresponds to the grand canonical ensemble with chemical potential μ_q fixed, while $\varepsilon = 1$ corresponds to the canonical ensemble with charge density n_q fixed. We choose grand canonical ensemble ($\varepsilon = 0$) and put the solutions (3) into (A3) to obtain the on-shell Euclidean action $S^{(E)}_R[g_{\mu\nu}, A_\mu]$. Then, the free energy density turns out to be

$$\frac{\Omega_0}{V_2} = -\frac{T}{V_2}\log Z_R = \frac{T}{V_2} S^{(E)}_R[g, A_\mu] = -\frac{r_h^3}{2\kappa^2 L^4}\left(1 + \frac{L^4}{g_F^2}\frac{\mu_q^2}{r_h^2}\right), \tag{A5}$$

where V_2 is the volume of the boundary system labelled by (x, y).

When a system is in thermal equilibrium in a certain phase, the following thermodynamic relation is satisfied:

$$\mathcal{E} + \mathcal{P} = Ts + \mu_q n_q. \tag{A6}$$

And the energy density and pressure of a conformal matter are

$$\mathcal{E} = \mathcal{T}^t_t, \qquad \mathcal{P} = \mathcal{T}^x_x, \qquad \mathcal{E} = 2\mathcal{P}. \tag{A7}$$

Using the above thermodynamic relations, one obtains the free energy of the background gravity

$$\Omega_R/V_2 \equiv \mathcal{E} - Ts - \mu_q n_q = -\mathcal{P}. \tag{A8}$$

Let us consider the simplest case for now. The free energy contributed by a neutral scalar field Ψ at the probe limit is

$$S_{\mathcal{M}}^{(E)} = -\frac{V_2}{T}\left[\int_{r_h}^{\infty} \mathrm{d}r\sqrt{g}\mathcal{L}_\Psi + \sqrt{\gamma}\mathcal{L}_{\text{c.t.}}\right],$$
$$g_M^2\mathcal{L}_\Psi = -\frac{1}{2}(\partial\Psi)^2 - V(\Psi),$$
$$V(\Psi) = \frac{1}{2}m_\Psi^2|\Psi|^2 + \frac{1}{4}\lambda_\Psi|\Psi|^4, \tag{A9}$$

and $\mathcal{L}_{\text{c.t.}}$ is the boundary counterterm to make the on-shell action finite. The equation of motion for the neutral scalar field Ψ turns out to be

$$r^{-2}\partial_r[r^4 f(r)\partial_r\Psi] - m_\Psi^2 L^2\Psi - \lambda_\Psi L^2\Psi^3 = 0. \tag{A10}$$

If we consider the contribution of the self-interaction term $\lambda_\Psi|\Psi|^4$ in the Lagrangian density, the asymptotic behavior of the scalar field receives nontrivial correction as follows:

$$\Psi \to \frac{J_\Psi}{r^{\Delta_\Psi^-}} + \frac{O_\Psi}{r^{\Delta_\Psi^+}} + \frac{\gamma}{r^{3\Delta_\Psi^-}} + \cdots, \qquad \gamma = \frac{\lambda_\Psi J_\Psi^3}{2\Delta_\Psi^-(4\Delta_\Psi^- - 3)}, \tag{A11}$$

$$\Delta_\Psi^\pm = \frac{3}{2} \pm \nu_\Psi, \qquad \nu_\Psi = \sqrt{\frac{9}{4} + m_\Psi^2}. \tag{A12}$$

In the case of $3\Delta_\Psi^- > \Delta_\Psi^+$, i.e. $m_\Psi^2 < -27/16$, or $J_\Psi = 0$, the correction term in (A11) is of higher order in $1/r$ and can be ignored, and the standard quantization scheme is not altered. However, for $3\Delta_\Psi^- \le \Delta_\Psi^+$, the counterterm needs to be taken into account,

$$g_M^2\mathcal{L}_{\text{c.t.}} = \frac{\Delta_\Psi^-}{2L}\Psi^2 + \frac{\lambda_\Psi L}{4(4\Delta_\Psi^- - 3)}\Psi^4 + \cdots, \tag{A13}$$

to make the on-shell action finite at high energy scale.

Considering the (A10), the on-shell action for the neutral scalar field Ψ turns out to be

$$\mathcal{L}_\Psi = -\frac{1}{2g_M^2}\left[\nabla_\mu(\Psi\nabla^\mu\Psi) - \frac{1}{2}\lambda_\Psi\Psi^4\right]. \tag{A14}$$

Considering the background metric in (3), we obtain

$$-\int_{r_h}^{\infty}\mathrm{d}r\sqrt{g}\mathcal{L}_\Psi = \frac{1}{2g_M^2}\lim_{r\to\infty}\left[\frac{r^4}{L^4}f(r)(\Psi\partial_r\Psi)\right] - \frac{\lambda_\Psi}{4g_M^2}\left[\int_{r_h}^{\infty}\mathrm{d}r\frac{r^2}{L^2}\Psi^4\right]. \tag{A15}$$

Putting (A11) back into (A15), we have

$$-\int_{r_h}^{\infty}\mathrm{d}r\sqrt{g}\mathcal{L}_\Psi = \frac{1}{2g_M^2 L}\lim_{r\to\infty}\frac{r^3}{L^3}\left[-(J_\Psi)^2\Delta_\Psi^-\left(\frac{L}{r}\right)^{2\Delta_\phi^-} - 3J_\Psi O_\Psi\left(\frac{L}{r}\right)^3 - 3J_\Psi\gamma\Delta_\phi^-\left(\frac{L}{r}\right)^{4\Delta_\phi^-}\right] + \cdots. \tag{A16}$$

Following the procedure of holographic renormalization [60], we need to introduce the counterterms in (A13). The leading order expansions in the action are

$$\frac{\Delta_\Psi^-}{2L}\int\sqrt{h}\Psi^2 = \frac{1}{2L}\lim_{r\to\infty}\frac{r^3}{L^3}\left[(J_\Psi)^2\Delta_\Psi^-\left(\frac{L}{r}\right)^{2\Delta_\Psi^-} + 2\Delta_\Psi^- J_\Psi O_\Psi\left(\frac{L}{r}\right)^3 + 2J_\Psi\gamma\Delta_\Psi^-\left(\frac{L}{r}\right)^{4\Delta_\Psi^-}\right] + \cdots$$
$$\frac{\lambda_\Psi L}{4(4\Delta_\Psi^- - 3)}\int\sqrt{h}\Psi^4 = \frac{1}{2L}\lim_{r\to\infty}\frac{r^3}{L^3}\left[+J_\Psi\gamma\Delta_\phi^-\left(\frac{L}{r}\right)^{4\Delta_\Psi^-}\right] + \cdots \tag{A17}$$

Putting all of these terms into the total action (A9), we reach the finite formula of the on-shell Euclidean action. As a result, the free energy density becomes

$$\frac{\Delta\Omega_\Psi}{V_2} = \frac{1}{g_M^2}\left[-\nu_\Psi J_\Psi O_\Psi - \frac{\lambda_\Psi}{4}\int_{r_h}^{\infty}\mathrm{d}r\frac{r^2}{L^2}(\Psi^4) - \lim_{r\to\infty}\frac{\lambda_\Psi J_\Psi^4 L}{4(4\Delta_\Psi^- - 3)}\left(\frac{L}{r}\right)^{4\Delta_\Psi^- - 3}\right]. \tag{A18}$$

To keep our computation simple, we only consider the scalar field mass $m_\Psi^2 < -27/16$ or set $\lambda_\Psi = 0$. Therefore, the last term in (A18) drops out.

APPENDIX B: SCALING SYMMETRY IN THE HHH MODEL [37]

Here, we review a powerful scaling symmetry shown in Fig. 9 based on the HHH model [37]. In this model, not only the unbroken phase in Fig. 9 but also the symmetry breaking phase enjoy a scaling symmetry. This is more powerful than a typical field theory system with a quantum critical point where only the unbroken phase enjoys the scaling symmetry.

Consider a massive $U(1)$ charged scalar field Ψ coupled to a Maxwell field A in the gravitational background of Eq. (1). The dimensionless coupling is q_Ψ. To initiate the spontaneous symmetry breaking, it generally requires a nontrivial potential for Ψ. The simplest form is the Higgs-like potential $V(\Psi)$,

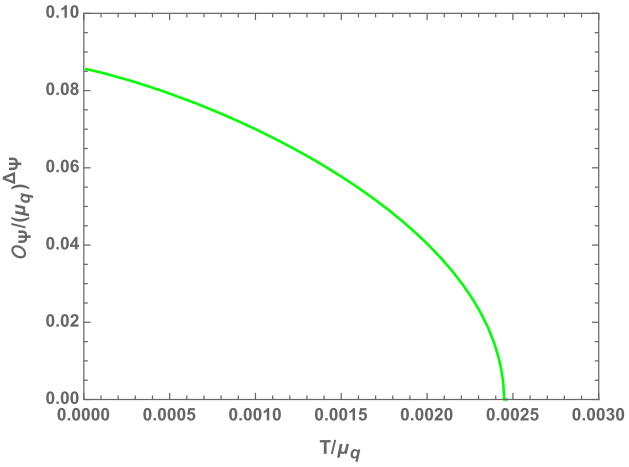

FIG. 9. The plot of expectation value O_Ψ vs the temperature T, at fixed chemical potential μ_q. Both of O_Ψ and T are rescaled by the appropriate power of chemical potential μ_q. The following parameters ate used: $J_\Psi = 0$, $m_\Psi^2 L^2 = -2.1$, $\lambda_\Psi = 1$ and $q_\Psi = 0.5$.

$$g_M^2 \mathcal{L}_M = g_M^2 \mathcal{L}_\Psi = -\frac{1}{2}|\partial\Psi - iq_\Psi A\Psi|^2 - V(\Psi),$$
$$V(\Psi) = \frac{1}{2}m_\Psi^2|\Psi|^2 + \frac{1}{4}\lambda_\Psi|\Psi|^4. \tag{B1}$$

(In the model of Ref. [37], $\lambda_\Psi = 0$.) For simplicity, we study the phase transition of Ψ in the probe limit, namely $2\kappa^2/g_M^2 \to 0$, such that the energy density of the fluctuations in Ψ is very small compared to that of the background. The symmetry broken phase boundary is obtained as the onset of the condensation of Ψ in the probe limit of the charged black brane background. The equation of motion is

$$\frac{1}{r^2L^2}\partial_r[r^4 f(r)\partial_r\Psi] - \left(m_\Psi^2 - \frac{L^2 q_\Psi^2 A_t(r)^2}{r^2 f(r)}\right)\Psi - \lambda_\Psi|\Psi|^2\Psi = 0. \tag{B2}$$

Note that near the boundary the last two terms are negligible compared with the first two terms. This implies a bigger symmetry near the boundary than near the black hole horizon.

Near the boundary, Ψ has the asymptotic behavior,

$$\Psi \to \frac{J_\Psi}{r^{\Delta_\Psi^-}} + \frac{O_\Psi}{r^{\Delta_\Psi^+}} + \cdots, \qquad \Delta_\Psi^\pm = \frac{3}{2} \pm \sqrt{\frac{9}{4} + m_\Psi^2 L^2}, \tag{B3}$$

where the standard quantization identifies J_Ψ as the source and O_Ψ as the vacuum expectation value in the dual boundary theory. Under the $r \to \lambda r$ scaling of Eq. (11), the asymptotic equation of motion remains invariant under the tranformation:

$$J_\Psi \to \lambda^{\Delta_\Psi^-} J_\Psi, \qquad O_\Psi \to \lambda^{\Delta_\Psi^+} O_\Psi. \tag{B4}$$

This implies that, once the O_Ψ vs T relation is known at certain chemical potential μ_q, its relation will be known to all μ_q as well.

Therefore, we can plot Fig. 9 in scaling invariant coordinates. Or we can replot it as Fig. 6 to show the scaling symmetry more explicitly. This scaling symmetry is so powerful that it involves not only the normal phase but also the symmetry breaking phase, which is not usually seen in condensed matter systems.

[1] J. Bardeen, L. N. Cooper, and J. R. Schrieffer, Microscopic theory of superconductivity, Phys. Rev. **106**, 162 (1957).
[2] J. Bardeen, L. N. Cooper, and J. R. Schrieffer, Theory of superconductivity, Phys. Rev. **108**, 1175 (1957).
[3] T. C. Ozawa and S. M. Kauzlarich, Chemistry of layered d -metal pnictide oxides and their potential as candidates for new superconductors, Sci. Technol. Adv. Mater. **9**, 033003 (2008).
[4] S. Sachdev, *Quantum Phase Transitions*, 2nd ed. (Cambridge University Press, Cambridge, England, 2011).
[5] S. Sachdev, What can gauge-gravity duality teach us about condensed matter physics?, Annu. Rev. Condens. Matter Phys. **3**, 9 (2012).
[6] G. G. Lonzarich, N. D. Mathur, F. M. Grosche, S. R. Julian, I. R. Walker, D. M. Freye, and R. K. W. Haselwimmer, Magnetically mediated superconductivity in heavy fermion compounds. Nature (London) **394**, 39 (1998).
[7] S. Sachdev and B. Keimer, Quantum criticality, Phys. Today **64** No. 2, 29 (2011).
[8] T. Moriya and K. Ueda, Spin fluctuations and high temperature superconductivity, Adv. Phys. **49**, 555 (2000).
[9] P. W. Anderson, The resonating valence bond state in La_2CuO_4 and superconductivity, Science **235**, 1196 (1987).
[10] Z. Y. Weng, Phase string theory for doped antiferromagnets, Int. J. Mod. Phys. B **21**, 773 (2007).
[11] E. Demler, W. Hanker, and S. C. Zhang, SO(5) theory of antiferromagnetism and superconductivity, Rev. Mod. Phys. **76**, 909 (2004).
[12] J. M. Maldacena, The large N limit of superconformal field theories and supergravity, Adv. Theor. Math. Phys. **2**, 231 (1998).

[13] S. S. Gubser, I. R. Klebanov, and A. M. Polyakov, Gauge theory correlators from noncritical string theory, Phys. Lett. B **428**, 105 (1998).
[14] E. Witten, Anti-de Sitter space and holography, Adv. Theor. Math. Phys. **2**, 253 (1998).
[15] M. Cubrovic, J. Zaanen, and K. Schalm, String theory, quantum phase transitions and the emergent Fermi-liquid, Science **325**, 439 (2009).
[16] T. Faulkner, H. Liu, J. McGreevy, and D. Vegh, Emergent quantum criticality, Fermi surfaces, and AdS(2), Phys. Rev. D **83**, 125002 (2011).
[17] K. Jensen, A. Karch, D. T. Son, and E. G. Thompson, Holographic Berezinskii-Kosterlitz-Thouless Transitions, Phys. Rev. Lett. **105**, 041601 (2010).
[18] N. Iqbal, H. Liu, M. Mezei, and Q. Si, Quantum phase transitions in holographic models of magnetism and superconductors, Phys. Rev. D **82**, 045002 (2010).
[19] E. Kiritsis and L. Li, Holographic competition of phases and superconductivity, J. High Energy Phys. 01 (2016) 147.
[20] P. Chaturvedi and P. Basu, Holographic quantum phase transitions and interacting bulk scalars, Phys. Lett. B **739**, 162 (2014).
[21] N. Iqbal, H. Liu, and M. Mezei, Quantum phase transitions in semilocal quantum liquids, Phys. Rev. D **91**, 025024 (2015).
[22] N. Iqbal, H. Liu, and M. Mezei, Lectures on holographic non-Fermi liquids and quantum phase transitions, arXiv:1110.3814.
[23] S. A. Hartnoll, Lectures on holographic methods for condensed matter physics, Classical Quantum Gravity **26**, 224002 (2009).
[24] S. S. Gubser, Breaking an Abelian gauge symmetry near a black hole horizon, Phys. Rev. D **78**, 065034 (2008).
[25] C.-L. Hung, X. Zhang, N. Gemelke, and C. Chin, Observation of scale invariance and universality in two-dimensional Bose gases, Nature (London) **470**, 236 (2011).
[26] X. Zhang, C.-L. Hung, S.-K. Tung, and C. Chin, Observation of quantum criticality with ultracold atoms in optical lattices, Science **335**, 6072 (2012).
[27] C. Varma, High-temperature superconductivity: Mind the pseudogap, Nature (London) **468**, 184 (2010).
[28] J. P. Gauntlett, J. Sonner, and T. Wiseman, Quantum Criticality and Holographic Superconductors in M-theory, J. High Energy Phys. 02 (2010) 060.
[29] P. Basu, J. He, A. Mukherjee, M. Rozali, and H. H. Shieh, Competing holographic orders, J. High Energy Phys. 10 (2010) 092.
[30] C. Y. Huang, F. L. Lin, and D. Maity, Holographic multiband superconductor, Phys. Lett. B **703**, 633 (2011).
[31] A. Donos, J. P. Gauntlett, J. Sonner, and B. Withers, Competing orders in M-theory: superfluids, stripes and metamagnetism, J. High Energy Phys. 03 (2013) 108.
[32] R. G. Cai, L. Li, L. F. Li, and Y. Q. Wang, Competition and coexistence of order parameters in holographic multi-band superconductors, J. High Energy Phys. 09 (2013) 074.
[33] W. Y. Wen, M. S. Wu, and S. Y. Wu, Holographic model of a two-band superconductor, Phys. Rev. D **89**, 066005 (2014).
[34] Z. Y. Nie, R. G. Cai, X. Gao, and H. Zeng, Competition between the s-wave and p-wave superconductivity phases in a holographic model, J. High Energy Phys. 11 (2013) 087.
[35] Z. Y. Nie and H. Zeng, P-T phase diagram of a holographic s + p model from Gauss-Bonnet gravity, J. High Energy Phys. 10 (2015) 047.
[36] R. G. Cai, R. Q. Yang, and F. V. Kusmartsev, Holographic model for antiferromagnetic quantum phase transition induced by magnetic field, Phys. Rev. D **92**, 086001 (2015).
[37] S. A. Hartnoll, C. P. Herzog, and G. T. Horowitz, Building a Holographic Superconductor, Phys. Rev. Lett. **101**, 031601 (2008).
[38] S. S. Gubser and S. S. Pufu, The gravity dual of a p-wave superconductor, J. High Energy Phys. 11 (2008) 033.
[39] S. A. Hartnoll, C. P. Herzog, and G. T. Horowitz, Holographic superconductors, J. High Energy Phys. 12 (2008) 015.
[40] M. Ammon, J. Erdmenger, M. Kaminski, and P. Kerner, Flavor superconductivity from gauge/gravity duality, J. High Energy Phys. 10 (2009) 067.
[41] R. G. Cai, L. Li, L. F. Li, and R. Q. Yang, Introduction to holographic superconductor models, Sci. China Phys. Mech. Astron. **58**, 060401 (2015).
[42] J. W. Chen, Y. J. Kao, D. Maity, W. Y. Wen, and C. P. Yeh, Towards a holographic model of D-wave superconductors, Phys. Rev. D **81**, 106008 (2010).
[43] F. Benini, C. P. Herzog, R. Rahman, and A. Yarom, Gauge gravity duality for d-wave superconductors: prospects and challenges, J. High Energy Phys. 11 (2010) 137.
[44] G. S. Hartnett and G. T. Horowitz, Geons and spin-2 condensates in the AdS soliton, J. High Energy Phys. 01 (2013) 010.
[45] K. Y. Kim and M. Taylor, Holographic d-wave superconductors, J. High Energy Phys. 08 (2013) 112.
[46] M. Baggioli and M. Goykhman, Phases of holographic superconductors with broken translational symmetry, J. High Energy Phys. 07 (2015) 035.
[47] M. Baggioli and M. Goykhman, Under the dome: Doped holographic superconductors with broken translational symmetry, J. High Energy Phys. 01 (2016) 011.
[48] F. Benini, C. P. Herzog, and A. Yarom, Holographic Fermi arcs and a d-wave gap, Phys. Lett. B **701**, 626 (2011).
[49] J. W. Chen, Y. S. Liu, and D. Maity, $d + id$ holographic superconductors, J. High Energy Phys. 05 (2011) 032.
[50] A. Salvio, Holographic superfluids and superconductors in dilaton-gravity, J. High Energy Phys. 09 (2012) 134.
[51] A. Salvio, Transitions in Dilaton Holography with Global or Local Symmetries, J. High Energy Phys. 03 (2013) 136.
[52] S. S. Gubser and F. D. Rocha, The Gravity Dual to a Quantum Critical Point with Spontaneous Symmetry Breaking, Phys. Rev. Lett. **102**, 061601 (2009).
[53] S. S. Gubser and A. Nellore, Ground states of holographic superconductors, Phys. Rev. D **80**, 105007 (2009).
[54] T. Nishioka, S. Ryu, and T. Takayanagi, Holographic superconductor/insulator transition at zero temperature, J. High Energy Phys. 03 (2010) 131.

[55] G. T. Horowitz and B. Way, Complete phase diagrams for a holographic superconductor/insulator system, J. High Energy Phys. 11 (2010) 011.

[56] G. T. Horowitz and M. M. Roberts, Zero temperature limit of holographic superconductors, J. High Energy Phys. 11 (2009) 015.

[57] M. Henningson and K. Skenderis, The holographic Weyl anomaly, J. High Energy Phys. 07 (1998) 023.

[58] V. Balasubramanian and P. Kraus, A stress tensor for Anti-de Sitter gravity, Commun. Math. Phys. **208**, 413 (1999).

[59] S. de Haro, S. N. Solodukhin, and K. Skenderis, Holographic reconstruction of space-time and renormalization in the AdS/CFT correspondence, Commun. Math. Phys. **217**, 595 (2001).

[60] K. Skenderis, Lecture notes on holographic renormalization, Classical Quantum Gravity **19**, 5849 (2002).